HHS Public Access

Author manuscript

Mucosal Immunol. Author manuscript; available in PMC 2017 June 19.

Published in final edited form as:

Mucosal Immunol. 2017 July ; 10(4): 936–945. doi:10.1038/mi.2016.99.

Microbiota induces tonic CCL2 systemic levels that control pDC trafficking in steady state

Melissa Swiecki[*,^], **Hannah Miller**[*], **Renata Sesti-Costa**[*], **Marina Cella**[*], **Susan Gilfillan**[*], and **Marco Colonna**[*]

[*]Department of Pathology and Immunology, Washington University School of Medicine, 425 S. Euclid Ave., St. Louis, MO 63110

[^]Janssen Research & Development LLC, Spring House, PA 19477

Abstract

Plasmacytoid dendritic cells (pDCs) detect viruses initiating antiviral IFN-I responses. The microbiota is known to shape immune responses, but whether it influences pDC homeostasis and/or function is poorly understood. By comparing pDCs in germ-free and specific pathogen-free mice, we found that the microbiota supports homeostatic trafficking by eliciting constitutive levels of the chemokine CCL2 that engages CCR2. Mononuclear phagocytes were required for tonic CCL2 levels. CCL2 was particularly important for trafficking of a $CCR2^{hi}$ subset of pDCs that produced proinflammatory cytokines and was prone to apoptosis. We further demonstrated that CCR2 was also essential for pDC migration during inflammation. Wildtype:$Ccr2^{-/-}$ mixed BM chimeras revealed that CCR2 promotes pDC migration in a cell-intrinsic fashion. Overall, we identify a novel role for the microbiota in shaping immunity, which includes induction of CCL2 at levels that control homeostatic trafficking of pDCs.

Keywords

plasmacytoid dendritic cell; CCR2; microbiota; germ-free; macrophage; monocyte

Introduction

Plasmacytoid dendritic cells (pDCs) are a subset of DC recognized for their ability to detect viral genomes through toll-like receptor (TLR) 7 and TLR9 and secrete large quantities of type I interferon (IFN-I), promoting early antiviral defense[1–3]. Unstimulated pDCs also contribute to immunological tolerance in steady state through multiple mechanisms. In contrast, inappropriately activated pDCs have been implicated in the pathogenesis of

Corresponding author: Marco Colonna, mcolonna@pathology.wustl.edu; Telephone: (314) 362-0367; FAX: (314) 747-0809.

Authors' contributions

MS, HM, RS-C performed experiments, SG established mice lines and colonies, MCe provided critical ideas, MS and MCo wrote the manuscript, MCo supervised research.

Disclosure

Melissa Swiecki is an employee of Janssen Research & Development LLC. The other authors declare no conflicts of interest.

autoimmune diseases characterized by an IFN-I signature such as systemic lupus erythematosus[2, 4].

pDCs have unique trafficking properties compared to conventional DC[2, 5]. pDCs are generated in the bone marrow (BM), circulate in the blood and reach lymphoid organs as well as non-lymphoid tissues in steady state. During inflammation, pDCs are part of the inflammatory infiltrate that extravasates from the blood vessels into sites of tissue damage and draining lymph nodes (LNs). pDC migration is controlled by multiple chemokine receptors and homing molecules. In steady state, CCR5 and, to a lesser extent, CCR2 promote pDC egress from the BM[6]. CD62L, CCR7 and CXCR4 mediate migration of pDCs into peripheral LNs and the splenic white pulp in steady state[2, 5]. CCR9 and its ligand CCL25 drive pDC migration to the thymus, where they transport peripheral antigens and induce tolerance[7]; CCR9 is also important for pDC recruitment to the small intestine[8]. Recently, it was shown that pDCs express MAdCAM-1 and β7 integrin which promote their trafficking into the intestinal intraepithelial compartment[9]. During inflammation, the ligands for E-selectin, β1 and β2 integrins, CXCR3, CCR5, CCR7 and the chemerin receptor ChemR23 drive pDC migration to sites of inflammation and draining LNs[2, 5]. A subset of human tonsil pDCs express CCR6 and CCR10, which enable them to migrate to inflamed epithelia in response to CCL20 and CCL27[10]. Additionally, pDCs have functional receptors for adenosine, C3a and C5a, which are released by damaged tissues[5]. Thus, a complex network of chemokines enables pDC trafficking in steady state and during disease.

The microbiota shapes mucosal and systemic immune responses by promoting homeostasis and function of many immune cell types including monocytes, granulocytes, DC, T cells and B cells[11–18]. However, whether and how the microbiota influences pDC homeostasis and functions remains largely unexplored. One study found that pDC frequencies and numbers were largely intact in germ-free (GF) mice, while mice bearing restricted enteric microbial communities had a dramatic reduction of pDCs in spleen and mesenteric LN (MLN)[19], suggesting a potential role for specific microbial communities in influencing pDC development and/or distribution. Moreover, commensal microbial products, such as polysaccharide A (PSA), influence pDC functions, endowing them with the capacity to promote the differentiation of IL-10 producing regulatory T cells[20]. Gut-associated pDCs are also capable of generating mucosal B cell responses[21, 22], promoting oral tolerance[23] and may influence Th17 generation[24].

Here, we analyzed pDCs in GF and specific pathogen free (SPF) mice and found that the microbiota was essential to sustain constitutive serum levels of CCL2 that promoted maintenance of pDCs in blood and peripheral tissues. Examination of pDCs subsets revealed that in SPF mice the ratio between $CCR2^{lo}$ and $CCR2^{hi}$ pDCs was approximately 2:1 in the BM and 1:1 in the periphery, whereas in GF mice the ratio was close to 2:1 also in the periphery, indicating a selective a reduction of peripheral $CCR2^{hi}$ pDCs. Functionally, $CCR2^{hi}$ pDCs were more prone to proinflammatory cytokine production, as well as spontaneous and glucocorticoid-induced apoptosis, compared to $CCR2^{lo}$ pDCs. GF mice also had reduced numbers of circulating $Ly6C^{hi}CD115^{+}$ inflammatory monocytes, which depend on CCR2 to exit the BM[25–27], thus supporting a general role for microbiota in the migration of $CCR2^{+}$ cells in steady state. The cell-intrinsic requirement for CCR2-CCL2

signaling for pDC trafficking in steady state was confirmed using WT:*Ccr2*$^{-/-}$ BM chimeras. Depletion experiments with clodronate (Clod) liposomes and anti-CSF-1R mAb revealed that mononuclear phagocytes were at least in part required for production of CCR2 ligands and pDC recruitment to LN in steady state. We further demonstrated that CCR2 was essential for pDC migration under inflammatory conditions. Taken together, our findings suggest a role of microbiota in inducing steady-state levels of CCL2, which is produced at least in part by mononuclear phagocytes and engenders homeostatic circulation of pDCs and inflammatory monocytes.

Results

Microbiota is required for homeostatic pDC distribution

To address the impact of microbiota on pDC homeostasis, we compared pDC frequencies and numbers in naïve SPF and GF mice. In steady state, peripheral blood pDCs were reduced in frequency and number in GF mice (Figure 1A). Peripheral blood monocytes were also markedly reduced (Figure 1A). Spleen, mesenteric lymph nodes (MLN), small intestine intraepithelial lymphocytes (IELs) and thymus from GF mice also revealed a reduction in pDCs (Figure 1B and 1C). To determine whether the defect in peripheral pDCs in GF mice was due to defective generation of pDCs in BM, we measured frequencies and numbers of mature and immature pDCs based on expression of Ly49Q and SiglecH. GF mice showed higher frequencies of mature pDCs (Ly49Q^{hi}SiglecH^{+}), immature pDCs (Ly49Q^{lo}SiglecH^{+}) and pDC progenitors (Ly49Q^{-}SiglecH^{+}) and higher absolute numbers of mature pDCs than SPF mice in the BM (Figure 1D and data not shown). Thus, these data suggested that the microbiota may promote egress of pDCs from BM.

Microbiota promotes trafficking of CCR2^{hi} pDCs through CCL2

It has been reported that pDC egress from BM in steady state depends on CCR5 and, in part, CCR2[6]. In C57BL/6 mice, pDCs uniformly express CCR5, whereas, based on the amount of CCR2 expressed, pDCs can be divided into two distinct subsets, CCR2^{lo} and CCR2^{hi} [6]. Thus, we sought to investigate whether lack of microbiota impairs pDC trafficking by affecting CCR5 and/or CCR2 expression. GF mice had normal levels of CCR5 on pDCs from BM, spleen and MLN (data not shown). However, we noted that the ratios of CCR2^{lo} and CCR2^{hi} pDCs differed between SPF and GF mice and that GF mice had a consistent reduction in CCR2^{hi} pDCs in the periphery (Figure 2A), suggesting a defective release of CCR2^{hi} pDCs from the BM. We further analyzed the systemic levels of CCR5 ligands (CCL4 and CCL5) and the CCR2 ligand CCL2 in SPF and GF mice. We found that CCL2 but not CCL4 or CCL5 was lower in GF mice (Figure 2B), suggesting that microbiota may be essential for constitutive production of CCL2 that promotes exit of CCR2^{hi} pDCs from the BM. To determine if CCL2 promotes pDC trafficking, mice were injected i.p. with recombinant CCL2 or PBS and pDC numbers in peritoneal exudate cells (PEC) were measured. Results showed an increase in pDC frequency and number in PEC, indicating that pDCs can be recruited by CCL2 (Figure 2C).

Because microbiota has been shown to promote tonic IFN-I signaling in mononuclear phagocytes[12, 28, 29] and IFN-I is required for pDC trafficking[30], we asked whether the

reduction of CCR2^{hi} pDCs in GF mice was related to impaired IFN-I signaling in pDCs. However, wildtype and *Ifnar*$^{-/-}$ mice had comparable frequencies of CCR2^{lo} and CCR2^{hi} pDCs in BM, spleen and MLN (Figure 2D). The importance of CCR9 in pDC trafficking has also been documented[7, 8]; therefore we evaluated CCR9 expression and systemic levels of CCL25 in SPF and GF mice. CCR9 expression was normal on pDCs from GF mice (Figure 2A) and serum CCL25 levels were comparable in SPF and GF mice (Figure 2B). Thus, these data suggested that the peripheral reduction of pDCs in GF mice, particularly the CCR2^{hi} subset, was due to lower levels of CCR2 ligands rather than defective expression of CCR5, CCR9 and their ligands or defective IFN-I signaling.

CCR2 deficiency affects pDC trafficking in steady state

To corroborate the role of CCR2 in pDC trafficking in steady state we examined *Ccr2*$^{-/-}$ mice[31]. We found that pDC frequencies and numbers in spleen and blood were reduced ~50% in *Ccr2*$^{-/-}$ mice (Figure 3A and 3B). To further demonstrate a role for CCR2 signaling in maintaining the CCR2^{hi} subset in the periphery, we examined a recently generated line of CCR2-eGFP gene-targeted reporter mice[32]. *Ccr2*$^{eGFP/+}$ mice harbored eGFP^{lo} and eGFP^{hi} pDCs subsets, which corresponded to those observed with CCR2 staining (Figure 3C and data not shown). In most compartments of *Ccr2*$^{eGFP/+}$ mice examined, the ratio of eGFP^{lo} to eGFP^{hi} pDCs was 1:1, while in the BM there was a trend toward more eGFP^{lo} than eGFP^{hi} pDCs (Figure 3C). However, more eGFP^{hi} pDCs were present in the BM of *Ccr2*$^{eGFP/eGFP}$ mice, which are deficient for CCR2, such that eGFP^{hi} and eGFP^{lo} pDCs were almost equally represented (Figure 3D); this implied that CCR2 signaling preferentially promotes homeostatic trafficking of CCR2^{hi} pDCs.

CCL2 levels were also elevated in *Ccr2*$^{eGFP/eGFP}$ mice (Figure 3E), probably due to reduced usage and subsequent degradation. *Ccr2* and *Ccr5* genes are adjacent to each other on chromosome 9. Because CCR5 plays a major role in pDC egress from BM in steady state[6], we verified that CCR5 expression levels on pDCs were normal in both *Ccr2*$^{-/-}$ and *Ccr2*$^{eGFP/eGFP}$ mice (data not shown). Furthermore, since CCR5 ligands are made by various cell types, some of which may be altered or absent in the periphery of *Ccr2*$^{-/-}$ mice, we investigated whether lack of CCR2 results in impaired production of CCR5 ligands. In fact, systemic levels of CCR5 ligands were higher in *Ccr2*$^{eGFP/eGFP}$ mice relative to *Ccr2*$^{eGFP/+}$ and WT mice (Figure 3E), indicating that CCR2 deficiency does not impair CCR5 signaling. Altogether, these results indicate that CCR2 deficiency leads to a reduction in peripheral pDCs.

Mononuclear phagocytes are required for production of CCR2 ligands and pDC homeostasis

CCL2 is produced by several cell types including mononuclear phagocytes and T cells and is rapidly expressed by BM mesenchymal and colonic stromal cells in response to circulating bacterial infection, TLR and NOD ligands[33, 34]. Because mononuclear phagocytes can produce CCL2 and are primed by microbiota[16, 28, 29, 33], we tested whether that they had a role in the production of CCR2 ligands that drive pDC trafficking in steady state. We injected WT C57BL/6 mice with liposomes containing phosphate buffered saline (PBS) or clodronate (Clod) to eliminate mononuclear phagocytes. Two days after liposome injection,

we observed a ~50% reduction in total cellularity and pDC numbers in spleens of Clod-treated mice (Figure 4A). The CCR2^{hi} pDC subset appeared to be most affected by Clod treatment (Figure 4B). Analyses of MLN and inguinal LN (ILN) from PBS and Clod-treated mice also revealed a reduction in pDCs, particularly the CCR2^{hi} subset (Figure 4C). Additionally, we measured CCR2 and CCR5 ligands in serum from PBS and Clod-treated mice and found that serum CCL2 was strongly reduced after Clod administration (Figure 4D), confirming the requirement of mononuclear phagocytes for homeostatic levels of CCL2.

Clod treatment also reduced serum CCL4 (Figure 4D). Since we previously reported that pDC depletion impacts CCL4 levels[35], it is possible that lower levels of CCL4 in Clod-treated mice were a consequence of reduced numbers of pDCs. In contrast, serum CCL3 and CCL5 were increased in Clod-treated mice (Figure 4D) perhaps because of reduced consumption by pDCs and mononuclear phagocytes, which express CCR5[36].

Because of the toxicity associated with Clod, we also evaluated pDC numbers and serum CCL2 levels in B57BL/6 mice treated with anti-CSF-1R mAb, which reduces some mononuclear phagocyte subsets[37]. Serum CCL2 levels and CCR2^{hi} pDCs in MLN were partially reduced (Figure 4E), although, in contrast to Clod treatment, anti-CSF-1R mAb did not significantly impact spleen or lymph node pDC numbers (data not shown). It is likely that the limited effect of anti-CSF-1R mAb treatment on CCL2 levels and pDC numbers is related to the incomplete depletion of monocytes and several tissue resident macrophage populations[37]. Altogether, these data demonstrate that mononuclear phagocytes are required for production of CCL2 that promotes pDC trafficking and distribution in steady state. We postulate that in steady state, CCL2 may be largely produced by mononuclear phagocytes of the gut. Supporting this hypothesis, we did not detect CCR2 expression on intestinal intraepithelial pDCs using anti-CCR2 Ab (data not shown), whereas we could clearly see both CCR2^{lo} and CCR2^{hi} pDCs in IEL from *Ccr2*$^{eGFP/+}$ mice (see Figure 3C). This result suggests that gut pDCs are exposed to a high concentration of CCL2, such that CCR2 is occupied, downregulated and therefore undetectable by cell surface staining.

CCR2 deficiency impacts pDC trafficking during inflammation

We next assessed the contribution of CCR2 in pDC recruitment under inflammatory conditions. We used a local inflammation model based on footpad injection with heat-killed *Mycobacterium tuberculosis* (Mtb), which causes rapid recruitment of pDCs to draining popliteal lymph nodes (DLN)[38, 39]. On the day of analysis, absolute numbers of cells from DLN of *Ccr2*$^{-/-}$ mice were comparable to WT mice (Figure 5A), but, as expected, *Ccr2*$^{-/-}$ mice had a major reduction in CD11b^{+}CD14^{+} cells (Figure 5B). pDC numbers were increased in DLN from both groups of mice relative to contralateral (CLN), but DLN from *Ccr2*$^{-/-}$ mice contained 50% less pDCs than DLN from WT mice (Figure 5C), suggesting the importance of CCR2 in pDC recruitment during inflammation.

pDC migration during inflammation is controlled by multiple chemokines, such as CCR5 ligands[5], which are made by a variety of cell types. Thus, it was possible that some of these cells may be altered or absent in the periphery of *Ccr2*$^{-/-}$ mice and that the pDC migration defect was secondary to a defect of another cell type or another chemokine. To exclude this

possibility, we measured serum levels of CCR5 ligands in WT and *Ccr2*$^{-/-}$ mice after Mtb injection. CCL5, CCL4, CCL3 and CCL2 levels in *Ccr2*$^{-/-}$ mice were similar to or higher relative to WT mice (Figure 5D). To further address whether the pDC deficit in *Ccr2*$^{-/-}$ mice was intrinsic or extrinsic, we generated WT and *Ccr2*$^{-/-}$ mixed BM chimeras using C57BL/6 mice as recipients. Mice were analyzed 8 wk after reconstitution under steady state and inflammatory conditions. In naïve mice, *Ccr2*$^{-/-}$ pDCs were reduced in spleen, thymus and MLN compared to WT pDCs but ratios of WT and *Ccr2*$^{-/-}$ pDCs were similar in BM (Figure 5E). After Mtb injection, DLN contained fewer *Ccr2*$^{-/-}$ pDCs (Figure 5E). Taken together, these data suggest that CCR2 deficiency affects pDC homing in steady state and during inflammation in a cell-intrinsic fashion.

CCR2^{hi} and CCR2^{lo} pDCs are functionally different

Finally, we sought to determine whether CCR2^{hi} and CCR2^{lo} pDCs that are differentially responsive to microbiota-induced CCL2 are phenotypically and/or functionally different. As pDCs develop in the BM through sequential maturation steps [40], we examined whether CCR2 levels correlate with pDC maturation in BM using markers such as SiglecH, CCR9 and Ly49Q (Figure 6A and data not shown). The majority of pDC precursors were CCR2^{lo} or eGFP^{lo} (80–90%); in comparison, 50–60% of mature pDCs were CCR2^{lo} or eGFP^{lo} (Figure 6A and data not shown). Moreover, Ki67, which is a marker of proliferative capacity, was less expressed in CCR2^{hi} pDCs compared to CCR2^{lo} pDCs in BM (Figure 6B). Thus, CCR2^{hi} pDCs have a more mature phenotype than CCR2^{lo} pDCs.

We next evaluated the ability of BM CCR2^{lo} and CCR2^{hi} pDCs to respond to TLR7/9 stimulation *ex vivo*. pDC subsets were sorted from BM of CCR2$^{eGFP/+}$ mice and cultured overnight with CpGA, CpGB, Imiquimod or murine cytomegalovirus (MCMV). CCR2^{lo} pDCs produced more IFN-α than CCR2^{hi} pDCs after stimulation with CpGA and MCMV, a feature of immature pDCs. In contrast, CCR2^{hi} pDCs produced more proinflammatory cytokines such as IL-6 in response to Imiquimod and CpGB, a feature of mature pDCs (Figure 6C). We also tested the susceptibility of BM CCR2^{lo} and CCR2^{hi} pDCs to spontaneous and glucocorticoid-induced apoptosis and found that CCR2^{hi} cells were more susceptible to both (Figure 6D). We finally asked if CCR2^{lo} and CCR2^{hi} pDCs differed in the periphery. Splenic CCR2^{lo} and CCR2^{hi} pDCs expressed similar levels of the markers: Sca1, CCR9, BST2, Ly6C, CD11c, CD127, CD62L, CD4, CD8, CCR7, CXCR3, CCR6, CCR5, CXCR2, CXCR4 (Figure 6E). However, CCR2^{hi} pDCs expressed less Ki67 and were more prone to apoptosis (Figure 6B **and data not shown**). Altogether, these results suggest that CCR2^{hi} pDCs are functionally different from CCR2^{lo} pDCs, are more capable of producing proinflammatory cytokines and are prone to apoptosis.

Discussion

Our study establishes a role for the microbiota in inducing homeostatic serum levels of CCL2 that control trafficking and peripheral distribution of pDCs in the steady state. The microbiota induces CCL2 by stimulating mononuclear phagocytes, though other cells may also contribute to CCL2 production. Although CCR2 is expressed on several immune cell types, our results indicate that CCL2 acts directly on pDCs. Homeostatic CCL2 chiefly

impacts the CCR2^{hi} subset of pDCs, which are more capable of producing proinflammatory cytokines and more prone to apoptosis than the CCR2^{lo} subset. Moreover, our study also demonstrates that CCR2 is an important chemokine receptor for controlling pDC migration during inflammation induced by products of pathogenic bacteria.

Colonization of the intestine with commensal microbes is essential for normal development and homeostasis of the cellular and humoral immune system[11–18]. Several studies have shown that the gut microbiota impacts antigen presenting cells and mononuclear phagocytes[29, 41]. Similarly, intestinal *Bacteroides fragilis*, Segmented Filamentous Bacteria and *Clostridia* drive differentiation of Th1, Th17 and Tregs, respectively[42–44]. Moreover, the gut microbiota is a major driving force for differentiation of mucosal plasma cells and IgA production[21, 45]. Microbiota has also been shown to induce intestinal epithelial cells to secrete chemokines, such as CXCR2 ligands, that attract mast cells into the intestine[46]. Recently, commensal-derived signals were shown to provide tonic stimulation that establishes the activation threshold of the innate immune system[28, 29]. Moreover, commensal microbial products, such as PSA, were found to endow pDCs with the capacity to induce IL-10 producing regulatory T cells[20]. Our study reveals a novel function of the microbiota in the induction of constitutive levels of CCL2, which promote the circulation and distribution of pDCs as well as CCR2^{+} inflammatory monocytes. While CCL2 has been shown to be a key chemokine in the recruitment of CCR2^{+} inflammatory monocytes, which are involved in the pathogenesis of multiple diseases[25, 47, 48], this is the first time that CCL2 is shown to be important in the steady-state circulation of pDCs. It will be important to determine whether CCL2 is induced by selective commensals. It is also noteworthy that lack of microbiota did not result in a general reduction of serum chemokines, as serum levels of CCL4, CCL5 and CCL25 were similar in GF and SPF mice. Thus, CCL2 is a distinctive product of host immune system-microflora interaction.

We envision that microbiota activates cells with a prominent capacity to secrete CCL2, particularly mononuclear phagocytes, although we do not exclude other cells, especially in the intestine, such as colonic stromal cells, which were found to produce CCL2 in response to pathogenic bacteria in a Nod2-dependent manner[34]. Supporting the role of intestinal mononuclear phagocytes in CCL2 production in response to microbiota priming, we did not detect CCR2 expression on gut pDCs using anti-CCR2 Ab (data not shown), whereas CCR2 mRNA was expressed as demonstrated by eGFP expression in gut pDCs from *Ccr2*$^{eGFP/+}$ mice. This discrepancy between mRNA and protein expression may indicate high concentrations of CCL2 in the gut, which downregulates CCR2 rendering it undetectable by cell surface staining. It is likely that mononuclear phagocytes are also necessary for CCL2 production during inflammation, acting directly at the site of inflammation. Here, CCL2 released by inflammatory monocytes may activate pDCs reaching the inflammatory site as well as CCR2^{+} endothelial cells, promoting pDC adhesion to the endothelium and transendothelial migration. A similar mechanism has been shown for monocyte-mediated recruitment of neutrophils during arthritis[49].

It was previously shown that pDCs include CCR2^{hi} and CCR2^{lo} subsets and that a partial defect of CCR2 expression secondary to Runx2-deficiency contributes to retention of pDCs in the BM[6]. Our study advances these observations demonstrating that CCL2 controlling

steady-state pDC circulation is dependent on microbiota and preferentially drives the trafficking of CCR2^{hi} pDCs. Moreover, we define functional differences between CCR2^{hi} and CCR2^{lo} subsets. CCR2^{hi} pDCs produce more proinflammatory chemokines and are prone to spontaneous and glucocorticoid-induced apoptosis, whereas CCR2^{lo} pDCs produce more IFN-I and express Ki67. Thus, it appears that expression level of CCR2 somewhat correlates with pDC maturation, although it remains unclear whether CCR2^{lo} and CCR2^{hi} cells develop through sequential maturation steps or are distinct subsets. In conclusion, our findings identify a novel role of microbiota in shaping the immune system, which consists of the induction of tonic levels of serum CCL2 that control trafficking and peripheral localization of pDCs.

Methods

Mice and Treatments

All animal studies were approved by the Washington University Animal Studies Committee. SPF Male and female C57BL/6 mice (CD45.2) were bred in house. Female C57BL/6 GF mice (7–9 wk old) were bred in house by the J. Gordon lab (Washington University, St. Louis, MO). Male and female *Ccr2*$^{-/-}$ mice (CD45.2) were either purchased from the Jackson Laboratory or bred at Washington University School of Medicine. Male C57BL/6 (CD45.1) mice were purchased from the Jackson Laboratory for mixed BM chimera experiments. *Ifnar*$^{-/-}$ mice were kindly provided by A. French (Washington University School of Medicine). CCR2-eGFP reporter mice were generated and bred at Washington University School of Medicine[32]. Liposomes containing PBS or Clod were generous gifts from the G. Randolph lab (Washington University, St. Louis, MO). Liposomes were injected i.v. 48 h prior to analysis. Anti-CSF-1R mAb (M279) was kindly provided by Dr. Wenjun Ouyang (Amgen Inc.). C57BL/6 WT mice were injected i.p. with 400 μg anti-CSF-1R mAb or isotype control antibody (rIgG1) every 3 days for a total of 7 doses. C57BL/6 mice were injected with 300 ng of recombinant CCL2 (R&D systems) or PBS i.p. every other day for a total of 3 doses. Mice were analyzed 14 hours after the final injection.

BM Chimeras

BM from 6 wk old *Ccr2*$^{-/-}$ mice (CD45.2) and C57BL/6 mice (CD45.1) was harvested from tibias and femurs. After RBC lysis, cells were counted and mixed at a 1:1 ratio then injected into lethally irradiated (1000 rad) C57BL/6 mice (CD45.2). 3×10^6 cells of each genotype were injected i.v. 8 h after irradiation. BM chimeras were analyzed 8 wk after reconstitution.

Inflammation Assay

C57BL/6 mice, *Ccr2*$^{-/-}$ mice and mixed BM chimeras were injected in the hind footpads with 500 μg of heat-killed Mtb (Difco) on days −2 and 0. Serum, CLN and DLN were collected on day 1 for analysis.

Cell Preparations

Cell suspensions of spleen, thymus and LN were prepared by collagenase D digestion and passage through nylon mesh cell strainers (BD Biosciences). BM was collected from tibias and femurs. Whole blood was isolated by cardiac puncture for serum and flow cytometry.

Red blood cells were lysed with RBC lysis buffer (Sigma-Aldrich). Intraepithelial cells from small intestine were isolated as described with modifications[50]. Briefly, small intestines were sectioned after removal of Peyer's patches and incubated for 20 min at room temperature in HBSS, 10% bovine calf serum, EDTA and HEPES with mild agitation (two rounds). Supernatants were passed through nylon mesh strainers and centrifuged over a 44%-67% Percoll gradient.

Antibodies, Flow Cytometry and Sorting

The following reagents were from BD Biosciences, eBioscience or Biolegend: fluorochrome labeled anti-CD45.1 (A20), anti-CD45.2 (104), anti-CCR9 (eBioCW-1.2), anti-CD11c (HL3), anti-SiglecH (551 or 440c), anti-B220 (RA3-6B2), anti-CD4 (GK1.5), anti-CD8α (53-6.7), anti-CD11b (M1/70), anti-Ly6C (AL-21), anti-CD14 (Sa2-8), anti-CD62L (MEL-14), anti-CCR7 (4B12), anti-CCR6 (140706), anti-CCR5 (HM-CCR5), anti-CXCR4 (2B11/CXCR4), anti-CXCR2 (TG11/CXCR2), anti-CXCR3 (CXCR3-173), anti-BST2 (927), anti-CD127 (A7R34), anti-Sca1 (D7). Anti-Ly49Q (2E6) and anti-CCR2 (475301) were purchased from MBL or R&D Systems, respectively. Fc receptors were blocked before surface staining and dead cells were excluded with propidium iodide or by scatter. Staining for chemokine receptors, with the exception of CCR9, was achieved by incubating cells in complete medium containing Fc block and fluorochrome conjugated Abs for 30 min at 37°C. Flow cytometry data was analyzed with FlowJo software (Tree Star, Inc.). $CCR2^{hi}$ and $CCR2^{lo}$ pDCs from BM and spleens of WT or $CCR2^{eGFP/+}$ mice were sorted on a FACSAria (BD Biosciences).

Cell Culture and Stimulations

Primary cells were cultured in complete RPMI 1640 with 10% fetal calf serum (FCS), 1% glutamax, 1% nonessential amino acids, 1% sodium pyruvate, and 1% kanamycin sulfate (Gibco-Invitrogen). Sorted pDCs were stimulated overnight with CpGA 2216 (6 μg/ml, Operon); murine cytomegalovirus (MCMV, MOI 10:1); CpGB 1826 (6 μg/ml, Operon) or Imiquimod (6 μM, InvivoGen). For apoptosis studies, BM and spleen pDCs were incubated with medium alone or with 10^{-6} M methylprednisolone for 24 h. Apoptosis was assessed by Annexin-V and 7AAD staining. Proliferative capacity was measured by Ki67 staining.

ELISA and Cytometric Bead Array

Serum samples from mice were collected and stored at −20°C until analysis. IL-6, CCL2, CCL3, CCL4 and CCL5 were measured by cytometric bead array (BD Biosciences). CCL25 and IFN-α levels were measured by ELISA (Sigma-Aldrich and PBL Assay Science).

Statistical Analysis

The statistical significance of differences in mean values was analyzed with unpaired, two-tailed Student's t test. p values less than 0.05 were considered statistically significant.

Acknowledgments

We would like to thank Y. Wang, S. Rowland, A. French, T. Geurs, E. Unanue, B. Calderon, D. Kreisel, H. Hartzler, E. J. Pearce, W. Lam, G. Randolph, E. Gautier, S. Ivanov (Washington University, St. Louis, MO) for mice, reagents, injections and thoughtful discussions; J. I. Gordon, P. Ahern, D. O'Donnell and M. Karlsson (Center for

Genome Sciences & Systems Biology, Washington University, St. Louis, MO) for help with the experiments using GF mice; E. Lantelme and D. Brinja for cell sorting. M.S. was supported by K01DK095972 from NIDDK. Research reported in this publication was also funded by the National Institute of Arthritis and Musculoskeletal and Skin Diseases, part of the National Institutes of Health, under Award Number P30AR048335.

References

1. Iwasaki A, Medzhitov R. Control of adaptive immunity by the innate immune system. Nat. Immunol. 2015; 16:343–353. [PubMed: 25789684]
2. Swiecki M, Colonna M. The multifaceted biology of plasmacytoid dendritic cells. Nat. Rev. Immunol. 2015; 15:471–485. [PubMed: 26160613]
3. Reizis B, Bunin A, Ghosh HS, Lewis KL, Sisirak V. Plasmacytoid Dendritic Cells: Recent Progress and Open Questions. Ann. Rev. Immunol. 2011; 29:163–183. [PubMed: 21219184]
4. Ganguly D, Haak S, Sisirak V, Reizis B. The role of dendritic cells in autoimmunity. Nat. Rev. Immunol. 2013; 13:566–577. [PubMed: 23827956]
5. Sozzani S, Vermi W, Del Prete A, Facchetti F. Trafficking properties of plasmacytoid dendritic cells in health and disease. Trends Immunol. 2010; 31:270–277. [PubMed: 20579936]
6. Sawai CM, Sisirak V, Ghosh HS, Hou EZ, Ceribelli M, Staudt LM, et al. Transcription factor Runx2 controls the development and migration of plasmacytoid dendritic cells. J. Exp. Med. 2013; 210:2151–2159. [PubMed: 24101375]
7. Hadeiba H, Lahl K, Edalati A, Oderup C, Habtezion A, Pachynski R, et al. Plasmacytoid dendritic cells transport peripheral antigens to the thymus to promote central tolerance. Immunity. 2012; 36:438–450. [PubMed: 22444632]
8. Wendland M, Czeloth N, Mach N, Malissen B, Kremmer E, Pabst O, et al. CCR9 is a homing receptor for plasmacytoid dendritic cells to the small intestine. Proc. Natl. Acad. Sci. USA. 2007; 104:6347–6352. [PubMed: 17404233]
9. Clahsen T, Pabst O, Tenbrock K, Schippers A, Wagner N. Localisation of dendritic cells in the gut epithelium requires MAdCAM-1. Clin. Immunol. 2014; 156:74–84. [PubMed: 25464027]
10. Sisirak V, Vey N, Vanbervliet B, Duhen T, Puisieux I, Homey B, et al. CCR6/CCR10-mediated plasmacytoid dendritic cell recruitment to inflamed epithelia after instruction in lymphoid tissues. Blood. 2011; 118:5130–5140. [PubMed: 21937703]
11. Rescigno M. Intestinal microbiota and its effects on the immune system. Cell. Microbiol. 2014; 16:1004–1013. [PubMed: 24720613]
12. Cho H, Kelsall BL. The role of type I interferons in intestinal infection, homeostasis, and inflammation. Immunol. Rev. 2014; 260:145–167. [PubMed: 24942688]
13. Littman DR, Pamer EG. Role of the commensal microbiota in normal and pathogenic host immune responses. Cell Host & Microbe. 2011; 10:311–323. [PubMed: 22018232]
14. Kamada N, Seo SU, Chen GY, Nunez G. Role of the gut microbiota in immunity and inflammatory disease. Nat. Rev. Immunol. 2013; 13:321–335. [PubMed: 23618829]
15. Hooper LV, Littman DR, Macpherson AJ. Interactions between the microbiota and the immune system. Science. 2012; 336:1268–1273. [PubMed: 22674334]
16. Bain CC, Bravo-Blas A, Scott CL, Gomez Perdiguero E, Geissmann F, Henri S, et al. Constant replenishment from circulating monocytes maintains the macrophage pool in the intestine of adult mice. Nat. Immunol. 2014; 15:929–937. [PubMed: 25151491]
17. Balmer ML, Schurch CM, Saito Y, Geuking MB, Li H, Cuenca M, et al. Microbiota-Derived Compounds Drive Steady-State Granulopoiesis via MyD88/TICAM Signaling. J. Immunol. 2014; 193:5273–5283. [PubMed: 25305320]
18. Niess JH, Adler G. Enteric flora expands gut lamina propria CX3CR1+ dendritic cells supporting inflammatory immune responses under normal and inflammatory conditions. J. Immunol. 2010; 184:2026–2037. [PubMed: 20089703]
19. Fujiwara D, Wei B, Presley LL, Brewer S, McPherson M, Lewinski MA, et al. Systemic control of plasmacytoid dendritic cells by CD8+ T cells and commensal microbiota. J. Immunol. 2008; 180:5843–5852. [PubMed: 18424703]

20. Dasgupta S, Erturk-Hasdemir D, Ochoa-Reparaz J, Reinecker HC, Kasper DL. Plasmacytoid dendritic cells mediate anti-inflammatory responses to a gut commensal molecule via both innate and adaptive mechanisms. Cell Host & Microbe. 2014; 15:413–423. [PubMed: 24721570]
21. Tezuka H, Abe Y, Asano J, Sato T, Liu J, Iwata M, et al. Prominent role for plasmacytoid dendritic cells in mucosal T cell-independent IgA induction. Immunity. 2011; 34:247–257. [PubMed: 21333555]
22. Deal EM, Lahl K, Narvaez CF, Butcher EC, Greenberg HB. Plasmacytoid dendritic cells promote rotavirus-induced human and murine B cell responses. J. Clin. Invest. 2013; 123:2464–2474. [PubMed: 23635775]
23. Goubier A, Dubois B, Gheit H, Joubert G, Villard-Truc F, Asselin-Paturel C, et al. Plasmacytoid dendritic cells mediate oral tolerance. Immunity. 2008; 29:464–475. [PubMed: 18789731]
24. Li HS, Gelbard A, Martinez GJ, Esashi E, Zhang H, Nguyen-Jackson H, et al. Cell-intrinsic role for IFN-alpha-STAT1 signals in regulating murine Peyer patch plasmacytoid dendritic cells and conditioning an inflammatory response. Blood. 2011; 118:3879–3889. [PubMed: 21828128]
25. Auffray C, Sieweke MH, Geissmann F. Blood monocytes: development, heterogeneity, and relationship with dendritic cells. Ann. Rev. Immunol. 2009; 27:669–692. [PubMed: 19132917]
26. Serbina NV, Pamer EG. Monocyte emigration from bone marrow during bacterial infection requires signals mediated by chemokine receptor CCR2. Nat. Immunol. 2006; 7:311–317. [PubMed: 16462739]
27. Mildner A, Yona S, Jung S. A close encounter of the third kind: monocyte-derived cells. Advan. Immunol. 2013; 120:69–103. [PubMed: 24070381]
28. Abt MC, Osborne LC, Monticelli LA, Doering TA, Alenghat T, Sonnenberg GF, et al. Commensal bacteria calibrate the activation threshold of innate antiviral immunity. Immunity. 2012; 37:158–170. [PubMed: 22705104]
29. Ganal SC, Sanos SL, Kallfass C, Oberle K, Johner C, Kirschning C, et al. Priming of natural killer cells by nonmucosal mononuclear phagocytes requires instructive signals from commensal microbiota. Immunity. 2012; 37:171–186. [PubMed: 22749822]
30. Asselin-Paturel C, Brizard G, Chemin K, Boonstra A, O'Garra A, Vicari A, et al. Type I interferon dependence of plasmacytoid dendritic cell activation and migration. J. Exp. Med. 2005; 201:1157–1167. [PubMed: 15795237]
31. Boring L, Gosling J, Chensue SW, Kunkel SL, Farese RV Jr, Broxmeyer HE, et al. Impaired monocyte migration and reduced type 1 (Th1) cytokine responses in C-C chemokine receptor 2 knockout mice. J. Clin. Invest. 1997; 100:2552–2561. [PubMed: 9366570]
32. Epelman S, Lavine KJ, Beaudin AE, Sojka DK, Carrero JA, Calderon B, et al. Embryonic and adult-derived resident cardiac macrophages are maintained through distinct mechanisms at steady state and during inflammation. Immunity. 2014; 40:91–104. [PubMed: 24439267]
33. Shi C, Jia T, Mendez-Ferrer S, Hohl TM, Serbina NV, Lipuma L, et al. Bone marrow mesenchymal stem and progenitor cells induce monocyte emigration in response to circulating toll-like receptor ligands. Immunity. 2011; 34:590–601. [PubMed: 21458307]
34. Kim YG, Kamada N, Shaw MH, Warner N, Chen GY, Franchi L, et al. The Nod2 sensor promotes intestinal pathogen eradication via the chemokine CCL2-dependent recruitment of inflammatory monocytes. Immunity. 2011; 34:769–780. [PubMed: 21565531]
35. Swiecki M, Gilfillan S, Vermi W, Wang Y, Colonna M. Plasmacytoid dendritic cell ablation impacts early interferon responses and antiviral NK and CD8(+) T cell accrual. Immunity. 2010; 33:955–966. [PubMed: 21130004]
36. Gautier EL, Shay T, Miller J, Greter M, Jakubzick C, Ivanov S, et al. Gene-expression profiles and transcriptional regulatory pathways that underlie the identity and diversity of mouse tissue macrophages. Nat. Immunol. 2012; 13:1118–1128. [PubMed: 23023392]
37. Hume DA, MacDonald KP. Therapeutic applications of macrophage colony-stimulating factor-1 (CSF-1) and antagonists of CSF-1 receptor (CSF-1R) signaling. Blood. 2012; 119:1810–1820. [PubMed: 22186992]
38. Blasius A, Vermi W, Krug A, Facchetti F, Cella M, Colonna M. A cell-surface molecule selectively expressed on murine natural interferon-producing cells that blocks secretion of interferon-alpha. Blood. 2004; 103:4201–4206. [PubMed: 14695235]

39. Srivatsan S, Swiecki M, Otero K, Cella M, Shaw AS. CD2-associated protein regulates plasmacytoid dendritic cell migration, but is dispensable for their development and cytokine production. J. Immunol. 2013; 191:5933–5940. [PubMed: 24218450]
40. Reizis B. Regulation of plasmacytoid dendritic cell development. Curr. Op. Immunol. 2010; 22:206–211.
41. Diehl GE, Longman RS, Zhang JX, Breart B, Galan C, Cuesta A, et al. Microbiota restricts trafficking of bacteria to mesenteric lymph nodes by CX(3)CR1(hi) cells. Nature. 2013; 494:116–120. [PubMed: 23334413]
42. Mazmanian SK, Liu CH, Tzianabos AO, Kasper DL. An immunomodulatory molecule of symbiotic bacteria directs maturation of the host immune system. Cell. 2005; 122:107–118. [PubMed: 16009137]
43. Ivanov II, Atarashi K, Manel N, Brodie EL, Shima T, Karaoz U, et al. Induction of intestinal Th17 cells by segmented filamentous bacteria. Cell. 2009; 139:485–498. [PubMed: 19836068]
44. Atarashi K, Tanoue T, Shima T, Imaoka A, Kuwahara T, Momose Y, et al. Induction of colonic regulatory T cells by indigenous Clostridium species. Science. 2011; 331:337–341. [PubMed: 21205640]
45. Palm NW, de Zoete MR, Cullen TW, Barry NA, Stefanowski J, Hao L, et al. Immunoglobulin A coating identifies colitogenic bacteria in inflammatory bowel disease. Cell. 2014; 158:1000–1010. [PubMed: 25171403]
46. Kunii J, Takahashi K, Kasakura K, Tsuda M, Nakano K, Hosono A, et al. Commensal bacteria promote migration of mast cells into the intestine. Immunobiology. 2011; 216:692–697. [PubMed: 21281976]
47. Ingersoll MA, Platt AM, Potteaux S, Randolph GJ. Monocyte trafficking in acute and chronic inflammation. Trends Immunol. 2011; 32:470–477. [PubMed: 21664185]
48. Xiong H, Pamer EG. Monocytes and infection: modulator, messenger and effector. Immunobiology. 2015; 220:210–214. [PubMed: 25214476]
49. Wang B, Zinselmeyer BH, Runnels HA, LaBranche TP, Morton PA, Kreisel D, et al. In vivo imaging implicates CCR2(+) monocytes as regulators of neutrophil recruitment during arthritis. Cell. Immunol. 2012; 278:103–112. [PubMed: 23121982]
50. Lefrancois L, Lycke N. Isolation of mouse small intestinal intraepithelial lymphocytes, Peyer's patch, and lamina propria cells. Curr. Prot. Immunol. 2001:19. Chapter 3: Unit 3.

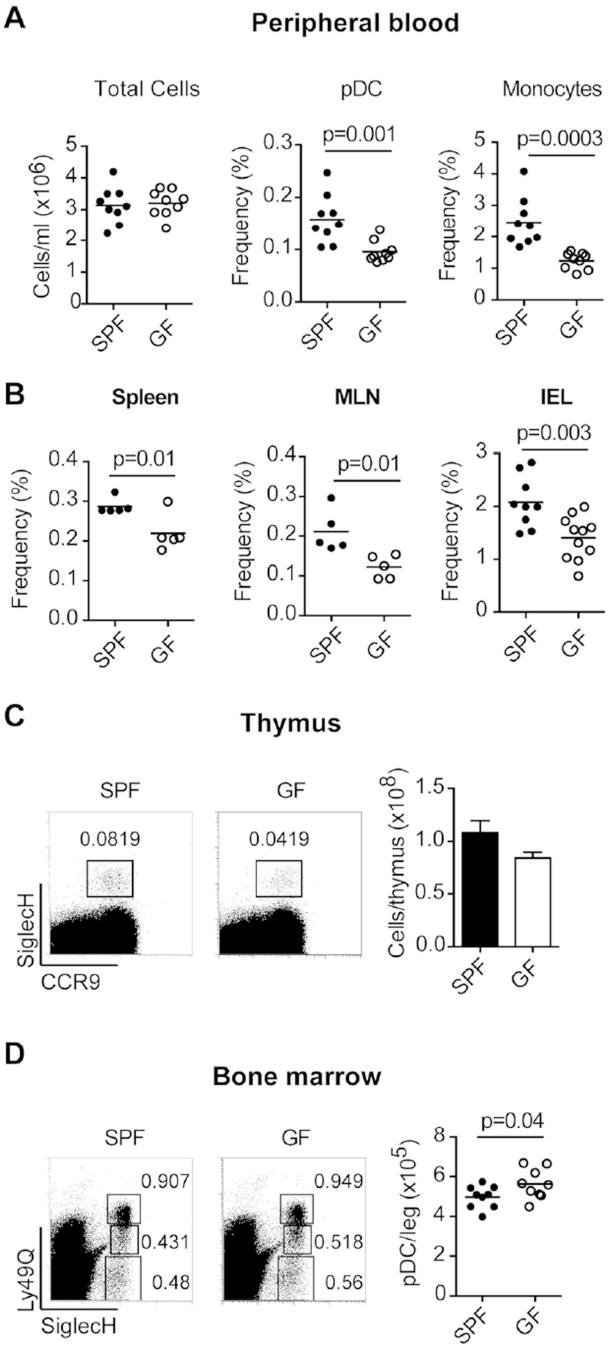

Figure 1. pDCs are reduced in the periphery of GF mice and accumulate in BM

(**A**) Peripheral blood from SPF and GF mice was analyzed for total numbers and frequencies of pDCs (SiglecH^{+}BST2^{+}) and monocytes (CD11b^{+}Ly6C^{+}CD115^{+}). (**B**) Frequencies of pDCs (CD45^{+}SiglecH^{+}BST2^{+}CCR9^{+}) in spleens, mesenteric lymph nodes (MLN) and small intestine IELs from SPF and GF mice. (**C**) Frequencies of thymic pDCs (SiglecH^{+}CCR9^{+}) and total numbers of live thymocytes in SPF and GF mice. Error bars represent the mean +/− SEM. (**D**) Frequencies and numbers of pDCs (Ly49Q^{hi}SiglecH^{+}) in BM of SPF and GF mice. Other gates show immature pDCs and pDC progenitors (Ly49Q^{int} and Ly49Q^{lo},

respectively). (**A-D**) Data are combined from or are representative of two or three independent experiments with 3–9 mice per experiment. p values indicate statistical significance.

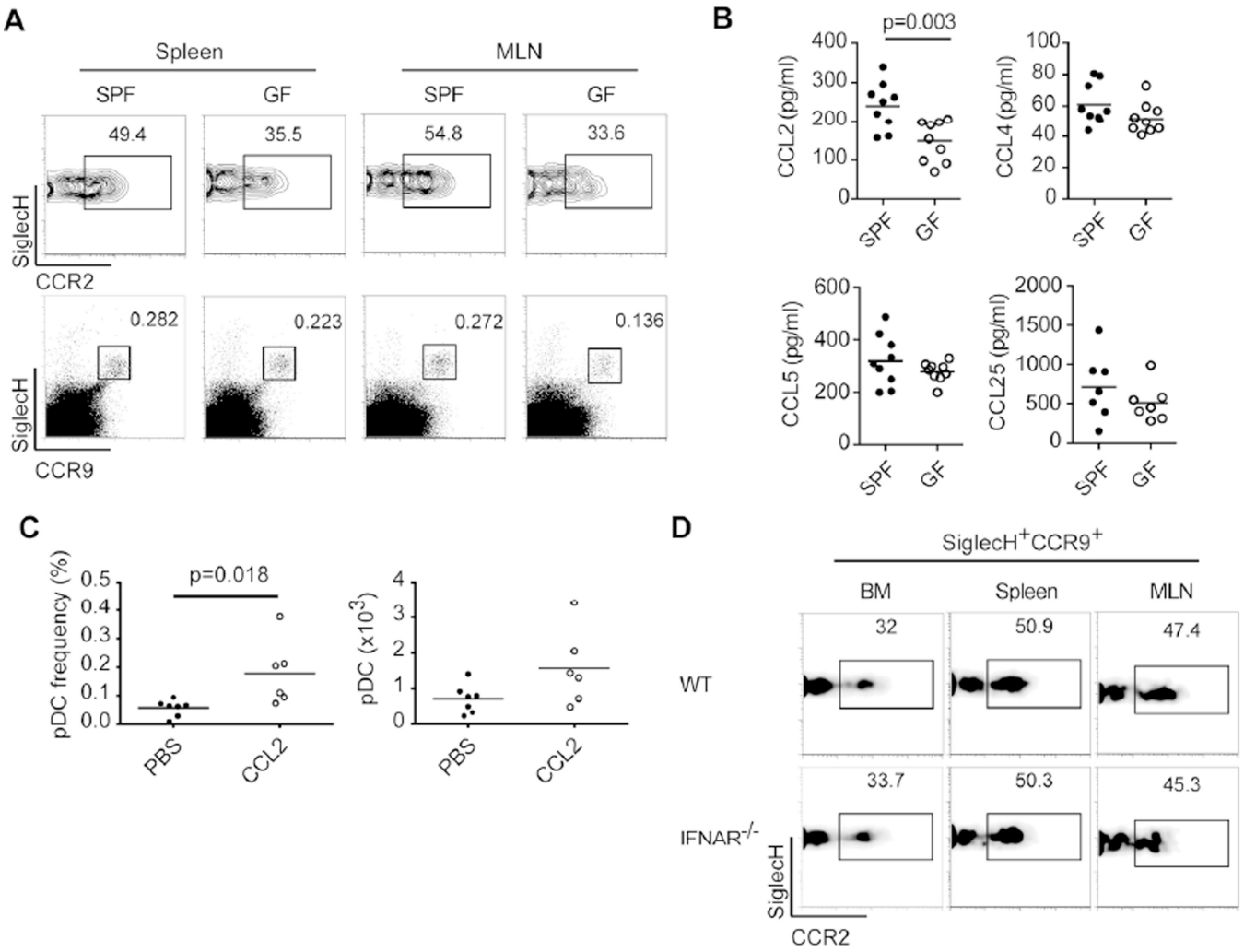

Figure 2. CCR2^{hi} pDCs and systemic levels of CCL2 are reduced in GF mice

(**A**) CCR2 expression on pDCs (SiglecH^{+}CCR9^{+}) from spleens and MLN of SPF and GF mice. (**B**) CCL2, CCL4, CCL5 and CCL25 levels in sera from SPF and GF mice. (**C**) C57BL/6 mice were injected i.p. with recombinant CCL2 or PBS and pDC frequencies and numbers were measured in PEC. (**D**) CCR2 expression on pDCs (SiglecH^{+}CCR9^{+}) from BM, spleen and MLN of WT and *Ifnar*$^{-/-}$ mice. (**A-D**) Data are combined from or are representative of two or three independent experiments with 2–9 mice per experiment. The p value indicates statistical significance.

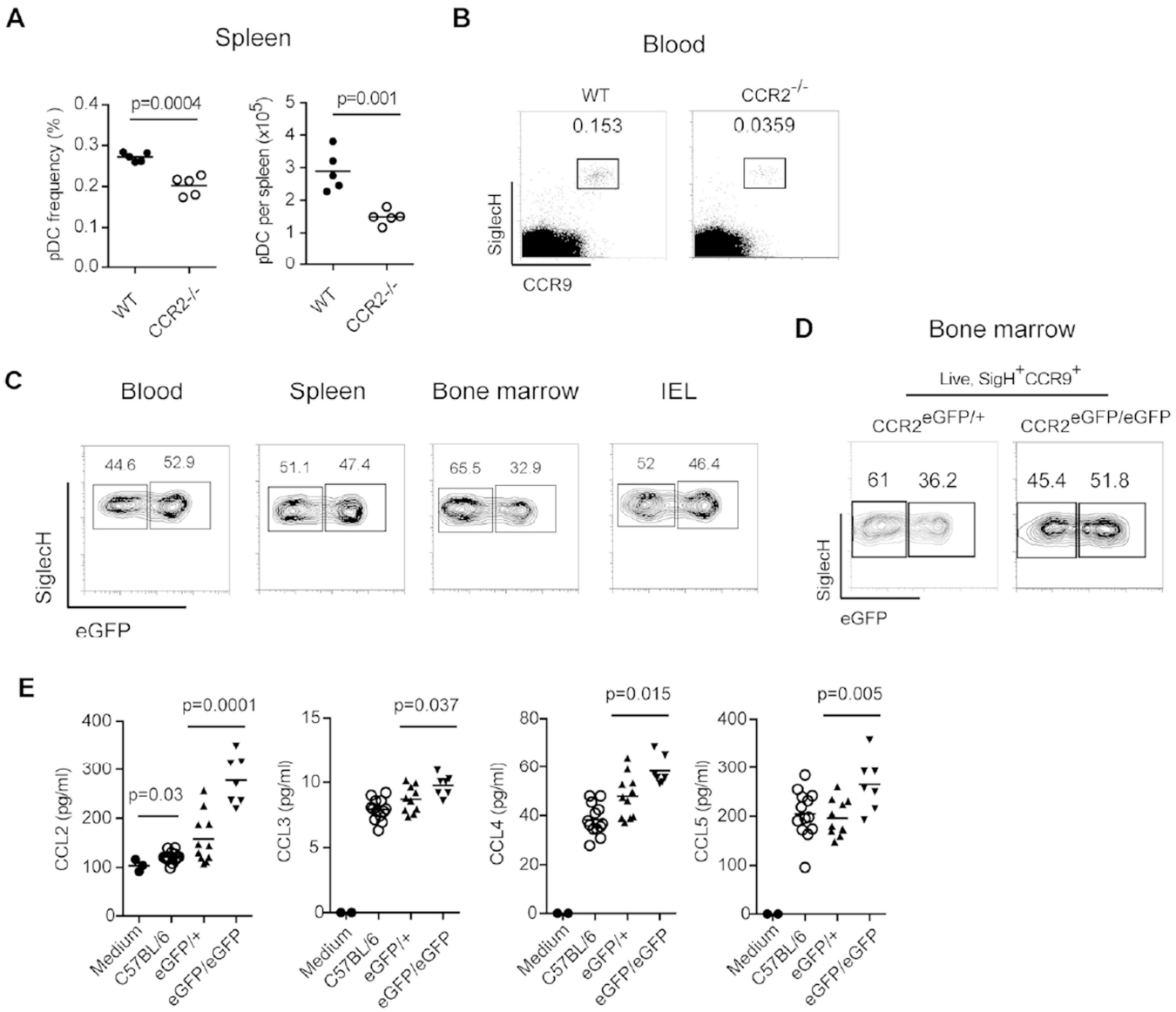

Figure 3. pDC homeostasis is altered in *Ccr2*$^{-/-}$ mice

(**A**) pDC frequencies (SiglecH^{+}CCR9^{+}) and numbers in spleens of C57BL/6 (WT) and *Ccr2*$^{-/-}$ mice. (**B**) Frequencies of pDCs (SiglecH^{+}CCR9^{+}) in peripheral blood from WT and *Ccr2*$^{-/-}$ mice. (**C**) Blood, spleen, BM and IELs were isolated from *Ccr2*$^{eGFP/+}$ mice and analyzed by flow cytometry. Graphs show two populations of SiglecH^{+}CCR9^{+} pDCs based on eGFP expression in all compartments. (**D**) Frequencies of eGFP^{lo} and eGFP^{hi} pDCs in BM of *Ccr2*$^{eGFP/+}$ and *Ccr2*$^{eGFP/eGFP}$ mice. (**E**) Systemic levels of CCL2, CCL3, CCL4 and CCL5 in WT, *Ccr2*$^{eGFP/+}$ and *Ccr2*$^{eGFP/eGFP}$ mice. Medium controls are included to indicate background. (**A-D**) Data are representative of two or three experiments with 3–5 mice per experiment. (**E**) Data are combined from two independent experiments (n=7–13). p values indicate statistical significance.

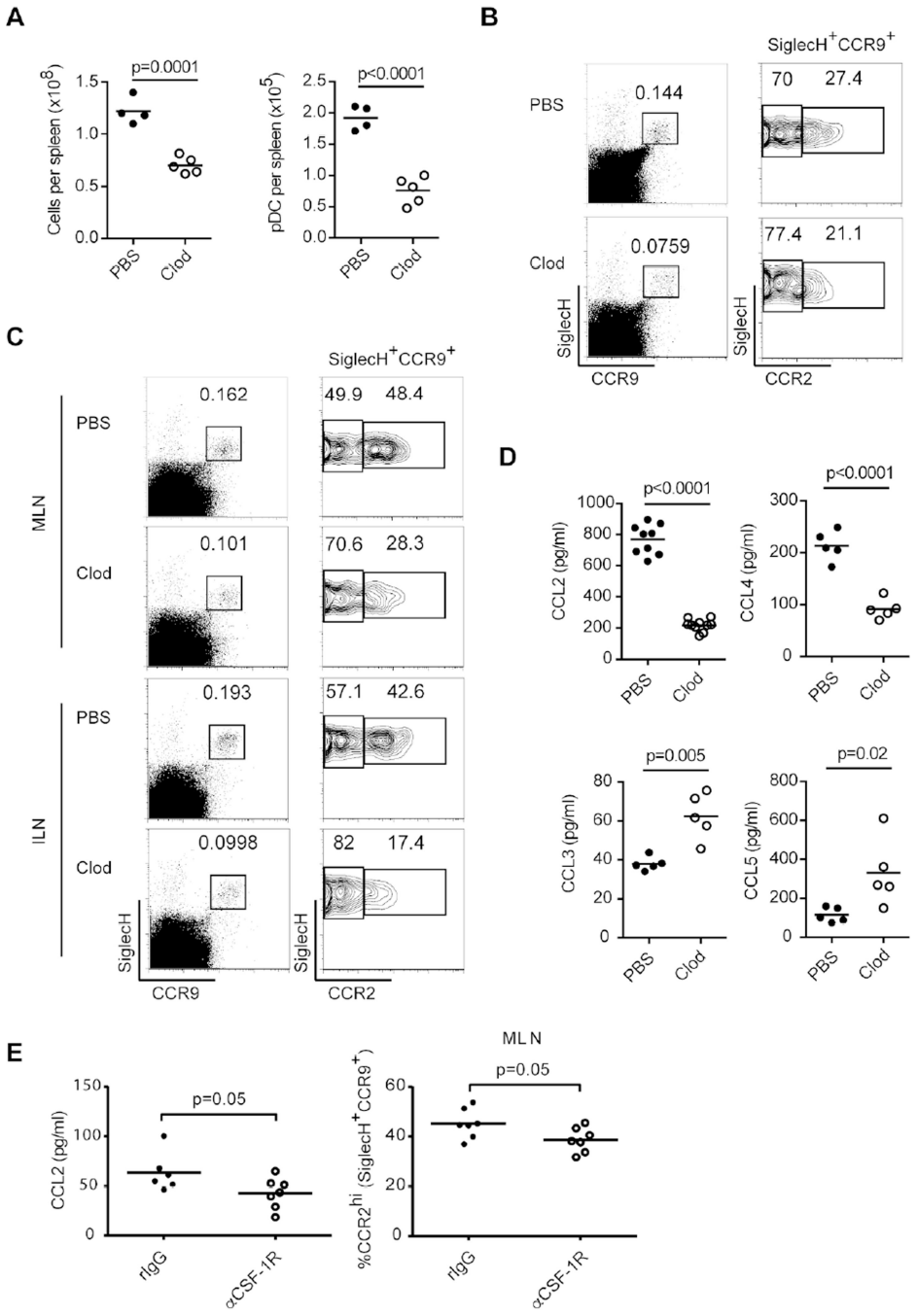

Figure 4. Mononuclear phagocytes produce CCR2 ligands and are required for pDC homeostasis

(**A-D**) C57BL/6 mice were injected i.v. with phosphate buffered saline (PBS) or clodronate (Clod) liposomes. Tissues and sera were analyzed 48 h post-injection. (**A**) Total cellularity and numbers of pDCs (SiglecH^{+}CCR9^{+}) in spleens. (**B**) Plots show frequencies of pDCs and frequencies of CCR2^{lo} and CCR2^{hi} pDC subsets in spleens. (**C**) Plots show frequencies of pDCs and CCR2^{lo} and CCR2^{hi} pDC subsets in MLN and ILN. (**D**) Systemic levels of CCL2, CCL3, CCL4 and CCL5. (**E**) C57BL/6 mice were injected i.p. with anti-CSF-1R mAb or isotype control antibody (rIgG1) every 3 days for a total of 7 doses. Mice were analyzed on

day 21. Graphs show serum levels of CCL2 and frequencies of $CCR2^{hi}$ pDCs in MLN. (**A-E**) Data are representative of two independent experiments with 2–9 mice per experiment. p values indicate statistical significance.

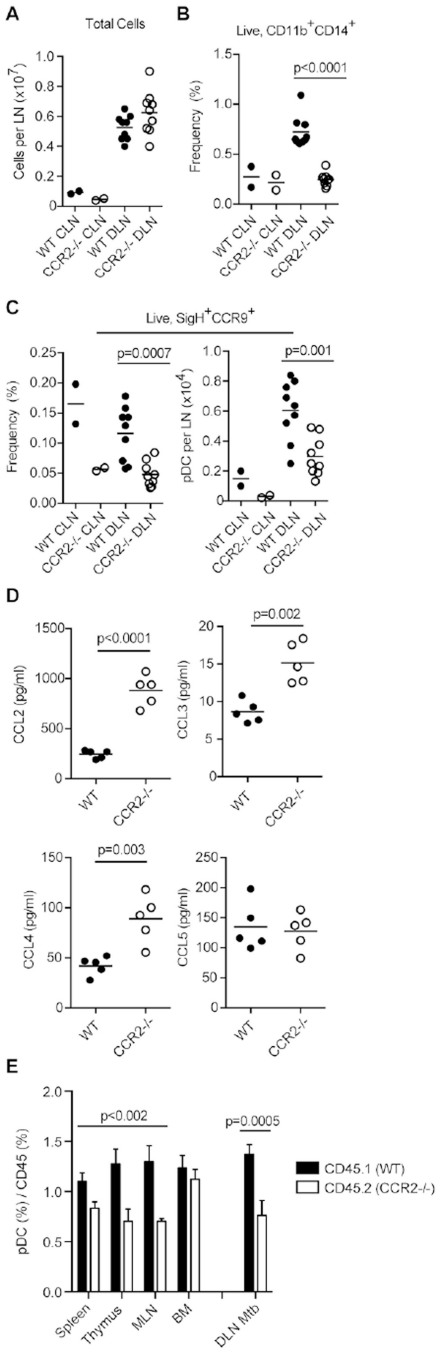

Figure 5. CCR2 deficiency impacts pDC recruitment during inflammation

(**A-D**) WT and *Ccr2*$^{-/-}$ mice were injected in the footpad with heat-killed *M. tuberculosis* (Mtb). (**A**) Total cells in contralateral (CLN) and draining (DLN) popliteal lymph nodes. (**B**) Frequencies of myeloid cells (CD11b^{+}CD14^{+}) in CLN and DLN. (**C**) Frequencies and numbers of pDCs (SiglecH^{+}CCR9^{+}) in CLN and DLN. (**D**) Systemic levels of CCL2, CCL3, CCL4 and CCL5 in WT and *Ccr2*$^{-/-}$ mice injected with Mtb. (**E**) Mixed BM chimeras were analyzed 8 wk after reconstitution for CD45.1^{+} (WT) and CD45.2^{+} (*Ccr2*$^{-/-}$) pDCs (SiglecH^{+}Ly49Q^{+}) in spleen, thymus, MLN and BM or in DLN after Mtb injection. Graphs

show the ratio of $CD45.1^+$ or $CD45.2^+$ pDCs (%) to total $CD45.1^+$ or $CD45.2^+$ cells (%). (**A-C**) Data are combined from two experiments with 4–5 mice per experiment. CLN were pooled from mice in each experiment (experiment one: n=4; experiment two: n=5). (**D**) Data are representative of two experiments with 4–5 mice per experiment. (**E**) Graphs show mean values +/− SD (n=4). p values indicate statistical significance.

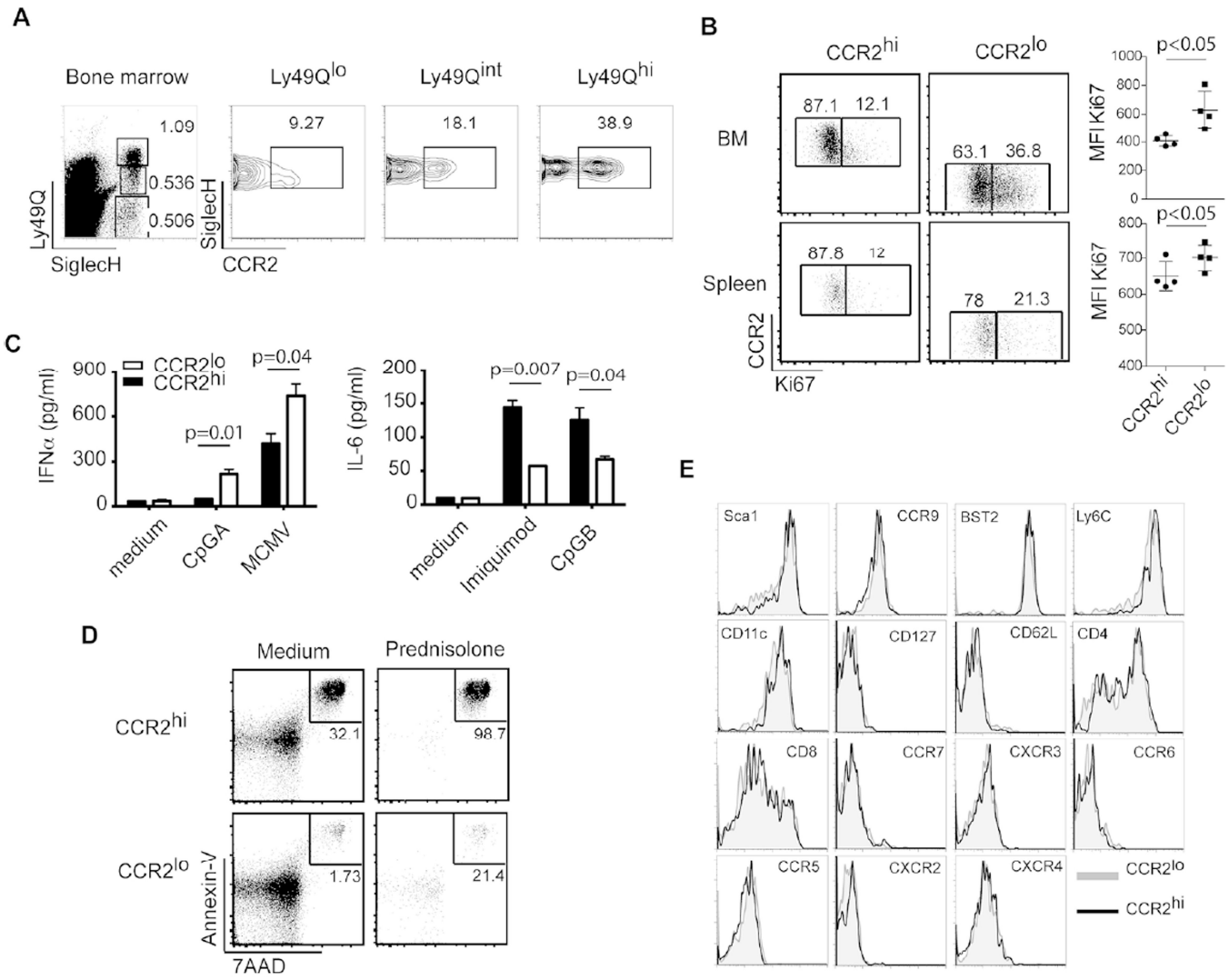

Figure 6. CCR2^{lo} and CCR2^{hi} pDCs are functionally distinct

(**A**) BM from C57BL/6 mice was stained for Ly49Q, SiglecH and CCR2. Graphs show percentages of CCR2^{lo} and CCR2^{hi} subsets in mature pDCs (Ly49Q^{hi}SiglecH^{+}), immature pDCs (Ly49Q^{int}SiglecH^{+}) and progenitors (Ly49Q^{lo}SiglecH^{+}). (**B**) BM and spleen cells were harvested and stained for Ki67 to measure proliferative capacity. Dot plots show CCR2^{hi} and CCR2^{lo} pDCs (SiglecH^{+}B220^{hi}) and graphs show mean fluorescence intensities (MFIs) of Ki67 expression. (**C**) CCR2^{lo} and CCR2^{hi} pDCs (CCR9^{+}SiglecH^{+}B220^{hi}) were sorted from BM of *Ccr2*$^{eGFP/+}$ mice and incubated with TLR agonists overnight. Supernatants were collected and analyzed for IFN-α and IL-6. Error bars represent the mean +/− SEM. (**D**) CCR2^{hi} and CCR2^{lo} pDCs (SiglecH^{+}B220^{hi}CD11c^{int}) were sorted from BM and incubated with either medium alone or with 10^{-6}M of methylprednisolone for 24 h. Apoptosis was measured by Annexin-V and 7AAD staining. (**E**) Phenotypic analysis of CCR2^{lo} and CCR2^{hi} pDCs from spleens of *Ccr2*$^{eGFP/+}$ mice. (**A-E**) Data are representative of two or three experiments with at least 3–5 mice per experiment. p values indicate statistical significance.